



*Supplement of*

## **Mass spectral characterization of secondary organic aerosol from urban cooking and vehicular sources**

**Wenfei Zhu et al.**

*Correspondence to:* Song Guo ([songguo@pku.edu.cn](mailto:songguo@pku.edu.cn))

The copyright of individual parts of the supplement might differ from the article licence.

6 **Contents:**

7 **Figure S1.** Schematic depiction of the simulation and measurement system for the cooking and vehicle  
8 experiments

9 **Figure.S2.** The mass spectra of aged HOA emission from different vehicle running conditions under  
10 different EPA.

11 **Figure.S3.** The mass spectra of aged COA emission from different Chinese dishes under different EPA.

12 **Figure.S4.** The changes in mass spectra of aged HOA emissions from different conditions.

13 **Figure.S5.** The mass spectra of aged COA oxidation under different OH exposure for different Chinese  
14 dishes.

15 **Figure.S6.** Van Krevelen diagram of POA, aged COA and aged HOA from vehicle and cooking.

16 **Figure.S7.** Diagnostic plots of the PMF analysis on OA mass spectral matrix for stir-frying cabbage.

17 **Figure.S8.** Mass spectra of the (a) 2-factor, and (b) 3-factor solution using PMF method in stir-frying  
18 cabbage OA analysis.

19 **Figure.S9.** Diagnostic plots of the PMF analysis on aged HOA mass spectral matrix for 2000rpm\_32Nm.

20 **Figure.S10.** Mass spectra of the (a) 2-factor, and (b) 3-factor solution using PMF method in  
21 2000rpm\_32Nm aged HOA analysis.

22 **Figure.S11.** The  $\theta$  angles between vehicle LO-SOA and MO-SOA under five running conditions.

23 **Figure.S12.** Mass spectral profiles of cooking POA, cooking SOA, vehicle LO-SOA, and vehicle MO-SOA  
24 as the primary and secondary spectrum constraints in ME-2 model.

25 **Figure.S13.** (a) 5-factor solution performed by ME-2 on organic mass spectra; (b) 7-factor solution  
26 performed by ME-2 on organic mass spectra during the wintertime in Shanghai.

27 **Figure.S14.** (a) 2-factor solution performed by PMF on organic mass spectra during the wintertime in  
28 Shanghai; (b) 4-factor solution performed by PMF on organic mass spectra during the wintertime in

29 Shanghai.

30 **Figure.S15.** Diagnostic plots of the PMF analysis on OA mass spectral matrix for the winter observation.

31 **Figure.S16.** Diagnostic plots of the PMF analysis on OA mass spectral matrix for the winter observation.

32 **Figure.S17.** The time-series correlations of all factors which resolved from PMF and ME-2 with external  
33 tracers during the wintertime observations in Shanghai.

34 **Figure.S18.** The time-series correlations of all factors which resolved from ME-2 constraining two POA  
35 profiles and ME-2 constraining four factors spectral profiles with external tracers during the wintertime  
36 observations in Shanghai.

37 **Figure.S19.** The comparison of the mass spectra, the diurnal variation, and fraction between ME-2  
38 constraining the spectral profiles of two primary factors (the cooking PMF POA, ambient HOA) and ME-2  
39 constraining four spectral profiles resolved factors during the wintertime in Shanghai.

40 **Figure.S20.** The comparison of the mass spectra, the diurnal variation, and fraction between ME-2 and PMF  
41 resolved factors during the summertime in Shanghai.

42 **Figure.S21.** The time-series correlations of all factors which resolved from PMF and ME-2 with external  
43 tracers during the summertime observations in Shanghai.

44

45 **Table S1.** Details of cooking and sampling procedures.

46 **Table S2.** Details of vehicle and sampling procedures.

47 **Table S3.** The OH exposure and photochemical age for all conditions in cooking and vehicle experiments

48 **Table S4.** The mass concentrations of primary organic aerosol (POA) for all conditions in vehicle  
49 experiments

50 **Table S5.** The  $\theta$  angles among the mass spectra of aged HOA under EPA 1.7 days, 2.9 days, and 4.1 days.

51 **Table S6.** The  $\theta$  angles among the mass spectra of POA and aged COA emission from different Chinese

dishes under EPA 0.3 day, 1.1 days, and 2.1 days.

**Table S7.** The  $\theta$  angles among the mass spectra under different EPA at one vehicle condition (1500rpm\_16Nm, 1750rpm\_16Nm, 2000rpm\_16Nm, 2000rpm\_32Nm, and 2000rpm\_40Nm, respectively).

**Table S8.** The  $\theta$  angles among the mass spectra under different EPA for different dishes.

**Table S9.** The optimum choices for PMF factors in stir-frying cabbage OA analysis.

**Table S10.** The optimum choices for PMF factors in 2000rpm\_32Nm aged HOA analysis.

**Table S11.** A summary of dominant peaks among cooking PMF POA.

**Table S12.** A summary of dominant peaks among cooking PMF SOA.

**Table S13.** A summary of dominant peaks among vehicle PMF LO-SOA.

**Table S14.** A summary of dominant peaks among vehicle PMF MO-SOA.

**Table S15.** The  $\theta$  angles among the mass spectra of cooking PMF SOA for different dishes.

**Table S16.** The  $\theta$  angles among the mass spectra of cooking PMF POA for different dishes.

**Table S17.** The  $\theta$  angles among the mass spectra of vehicle PMF LO-SOA at different conditions.

**Table S18.** The  $\theta$  angles among the mass spectra of vehicle PMF MO-SOA at different conditions.

**Table S19.** The  $\theta$  angles between ambient COA, HOA, LO-OOA and MO-OOA factors and the cooking PMF POA, SOA, and the vehicle PMF LO-SOA, MO-SOA.

**Table S20.** Pearson  $r$  between the factors identified by using PMF model (4-factor solution), and the external tracers during the wintertime observations in Shanghai.

**Table S21.** Descriptions of PMF solutions for organic aerosol in the winter study of Shanghai.

**Table S22.** Pearson  $r$  between the factors identified by using PMF and ME-2 model, and the external tracers during the wintertime observations in Shanghai.

**Table S23.** Pearson  $r$  between the factors identified by using PMF and ME-2 model, and the external tracers during the summertime observations in Shanghai.



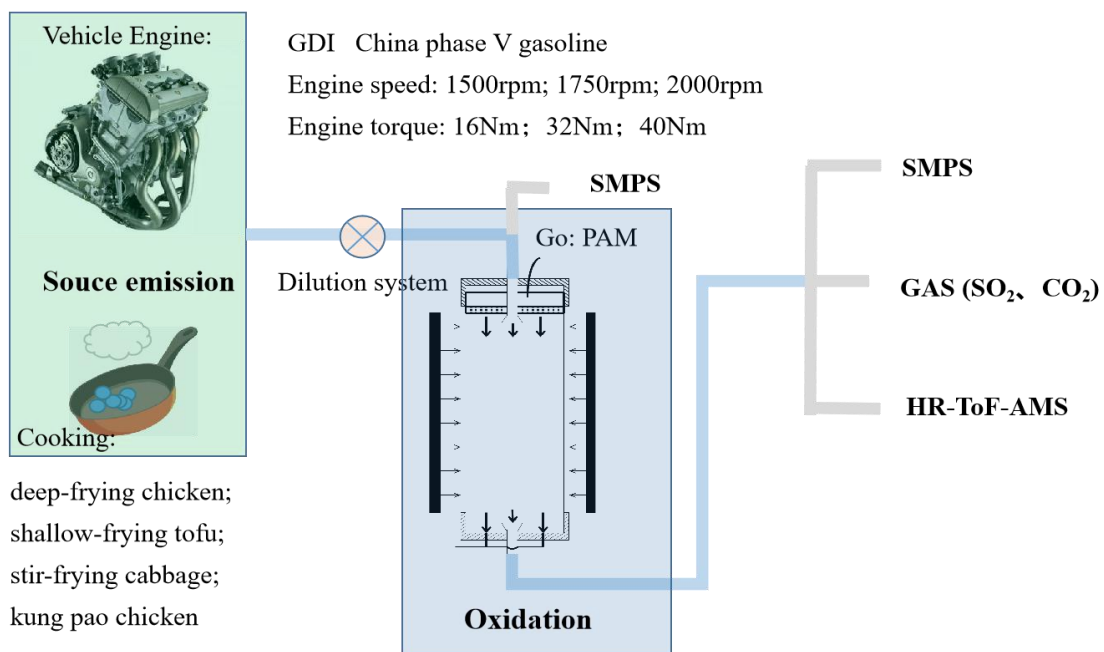


Fig.S1. Schematic depiction of the simulation and measurement system for the cooking and vehicle experiments.

82

83 Table S1. Details of cooking and sampling procedures.

Cooking Dish	Cooking Material	Oil Temperature	Cooking Time	Numbers for Each Dish	Sampling Time	Fuel	Sampling Temperate
Deep-fried chicken	170g chicken, 500ml corn oil	145~155°C	66 min	8	90 min		
Shallow-frying tofu	500g tofu, 200ml corn oil	100~110°C	64 min	8	60 min	Liquefied petroleum gas	20~25°C
Stir-frying cabbage	300g cabbage, 40ml corn oil	95~105°C	47 min	8	58 min	Iron work	
Kung Pao chicken	150g chicken, 50g peanut, 50g cucumber, 40ml corn oil	90~105°C	40 min	8	60 min		

84

85

86 Table S2. Details of vehicle and sampling procedures.

Running Condition		Sampling Time	Parallels	Fuel	Sampling Temperate
Rotating speed	Torque				
1500 rpm	16 Nm	60 min	5	Commercial China V gasoline	20~25°C
1750 rpm	16 Nm	60 min	5		
2000 rpm	16 Nm	60 min	5		
2000 rpm	32 Nm	60 min	5		
2000 rpm	40 Nm	60 min	5		

87

88

89

Table S3. The OH exposure and photochemical age for all conditions in cooking and vehicle experiments

Cooking experiment					Vehicle experiment				
O <sub>3</sub> concentration (ppbv)	RH (%) & Temperature (°C)	Description of Go: PAM	OH exposure (molecules cm <sup>-3</sup> s)	Photochemical Age (day)	O <sub>3</sub> concentration (ppbv)	RH (%) & Temperature (°)	Description of Go: PAM	OH exposure (molecules cm <sup>-3</sup> s)	Photochemical Age (day)
0		Sample flow	0	0	0		Sample flow	0	0
310		(7 L/min)	4.3E+10	0.3	624		(4 L/min) and	7.8E+10	0.6
1183	18~23%	and oxidant	9.6E+10	0.7	2367	44~49%	oxidant flow	2.1E+11	1.7
2217	& 16~19°C	flow (3	1.4E+11	1.1	4433	& 19~22°C	(1 L/min);	3.7E+11	2.9
4025		L/min); Residence time: 55 s	2.7E+11	2.1	6533		Residence time: 110 s	5.4E+11	4.2

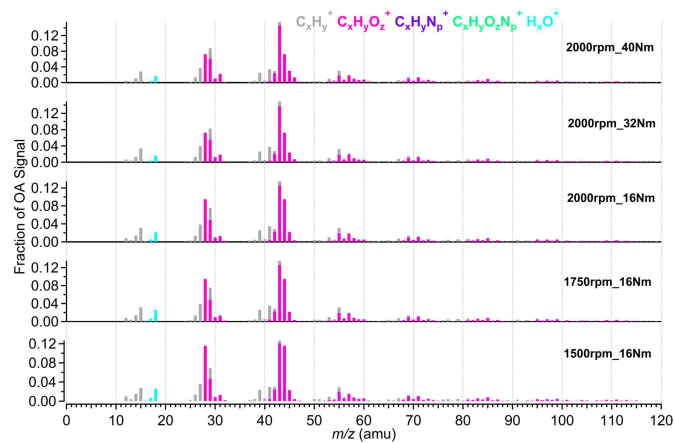
95

96 Table S4. The mass concentrations of primary organic aerosol (POA) for all conditions in vehicle experiments

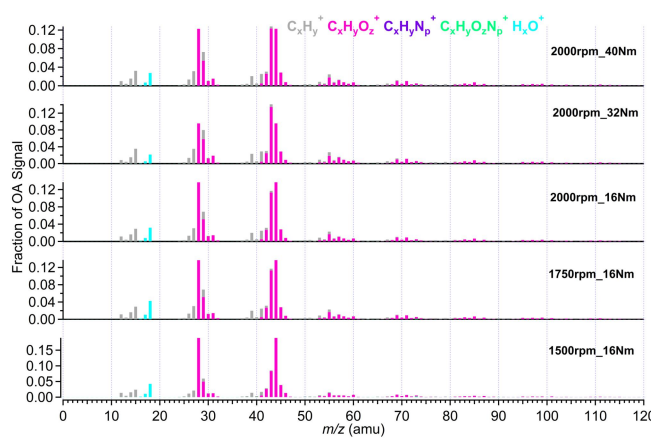
Experiment	POA Mass concentration ( $\mu\text{g}/\text{m}^3$ )	
	Average	Standard Deviation
1500rpm_16Nm	1.20	0.30
1750rpm_16Nm	1.26	0.61
2000rpm_16Nm	1.14	0.30
2000rpm_32Nm	1.29	0.62
2000rpm_40Nm	1.23	0.31

97

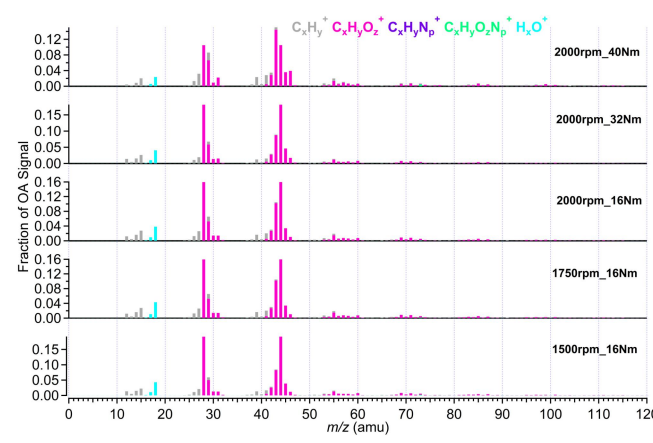
98



(a) EPA 1.7 days



(b) EPA 2.9 days



(c) EPA 4.1 days

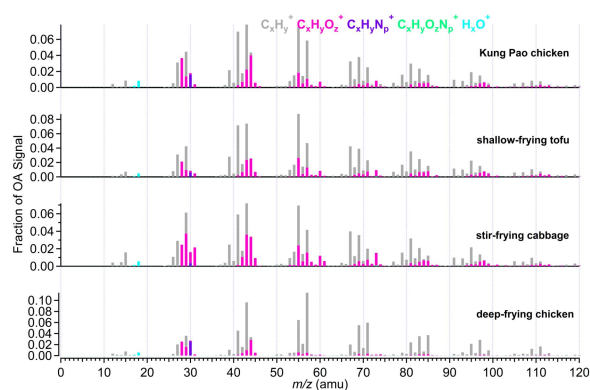
Fig.S2. The mass spectra of aged HOA emission from different vehicle running conditions under different EPA.

Table S5. The  $\theta$  angles among the mass spectra of aged HOA under EPA 1.7 days, 2.9 days, and 4.1 days.

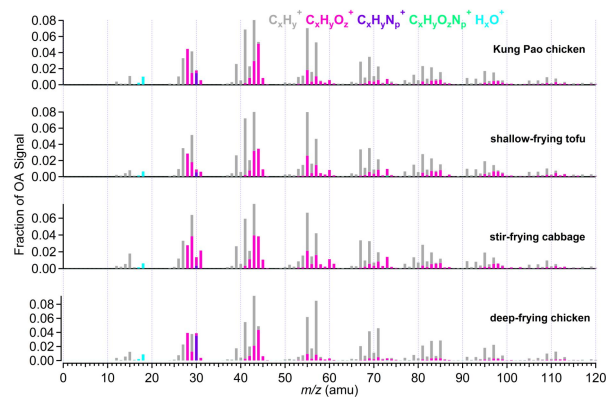
EPA1.7days $\theta$ angles	1500rpm_16Nm	1750rpm_16Nm	2000rpm_16Nm	2000rpm_32Nm	2000rpm_40Nm
1500rpm_16Nm	<b>0</b>	<b>8</b>	<b>8</b>	<b>16</b>	<b>18</b>
1750 rpm_16 Nm		<b>0</b>	<b>1</b>	<b>9</b>	<b>11</b>
2000 rpm_16 Nm			<b>0</b>	<b>9</b>	<b>11</b>
2000 rpm_32 Nm				<b>0</b>	<b>4</b>
2000 rpm_40 Nm					<b>0</b>

EPA2.9days $\theta$ angles	1500rpm_16Nm	1750rpm_16Nm	2000rpm_16Nm	2000rpm_32Nm	2000rpm_40Nm
1500rpm_16Nm	<b>0</b>	<b>14</b>	<b>14</b>	<b>29</b>	<b>19</b>
1750 rpm_16 Nm		<b>0</b>	<b>2</b>	<b>15</b>	<b>6</b>
2000 rpm_16 Nm			<b>0</b>	<b>14</b>	<b>5</b>
2000 rpm_32 Nm				<b>0</b>	<b>9</b>
2000 rpm_40 Nm					<b>0</b>

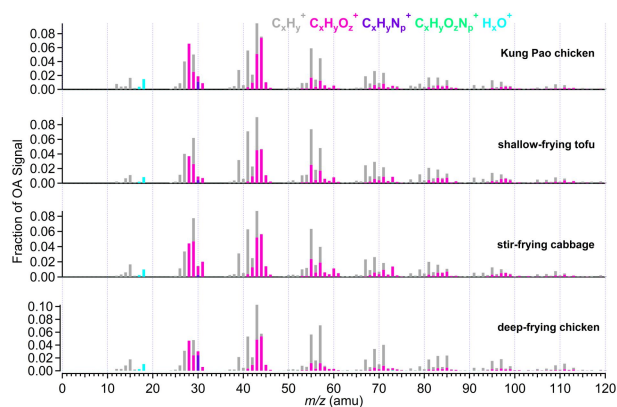
EPA4.1days $\theta$ angles	1500rpm_16Nm	1750rpm_16Nm	2000rpm_16Nm	2000rpm_32Nm	2000rpm_40Nm
1500rpm_16Nm	<b>0</b>	<b>8</b>	<b>8</b>	<b>3</b>	<b>29</b>
1750 rpm_16 Nm		<b>0</b>	<b>1</b>	<b>7</b>	<b>21</b>
2000 rpm_16 Nm			<b>0</b>	<b>7</b>	<b>21</b>
2000 rpm_32 Nm				<b>0</b>	<b>26</b>
2000 rpm_40 Nm					<b>0</b>



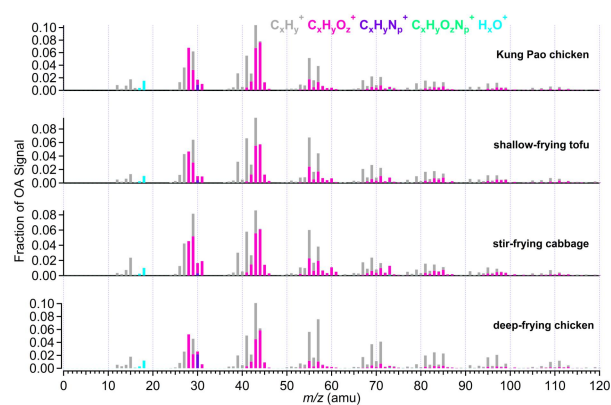
POA



EPA 0.3 days



EPA 1.1 days



EPA 2.1 days

Fig.S3. The mass spectra of aged COA emission from different Chinese dishes under different EPA.

110

111

112

Table S6. The  $\theta$  angles among the mass spectra of POA and aged COA emission from different Chinese dishes under EPA 0.3 day, 1.1 days, and 2.1 days.

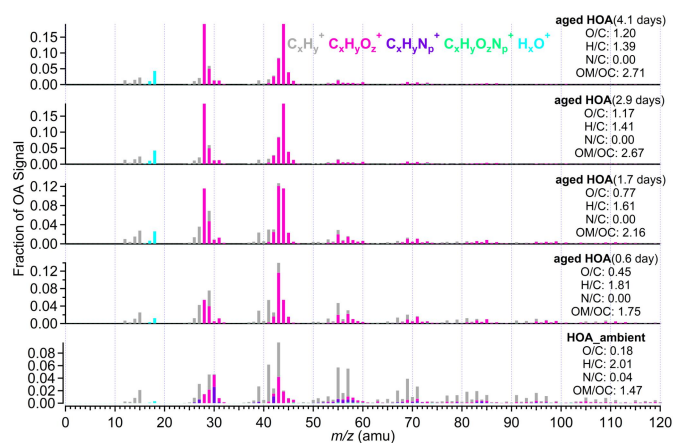
POA $\theta$ angles	deep-frying chicken	stir-frying cabbage	shallow-frying tofu	Kung Pao chicken
deep-frying chicken	<b>0</b>	<b>31</b>	<b>29</b>	<b>24</b>
stir-frying cabbage		<b>0</b>	<b>12</b>	<b>13</b>
shallow-frying tofu			<b>0</b>	<b>11</b>
Kung Pao chicken				<b>0</b>

EPA0.3 day $\theta$ angles	deep-frying chicken	stir-frying cabbage	shallow-frying tofu	Kung Pao chicken
deep-frying chicken	<b>0</b>	<b>23</b>	<b>22</b>	<b>17</b>
stir-frying cabbage		<b>0</b>	<b>10</b>	<b>13</b>
shallow-frying tofu			<b>0</b>	<b>10</b>
Kung Pao chicken				<b>0</b>

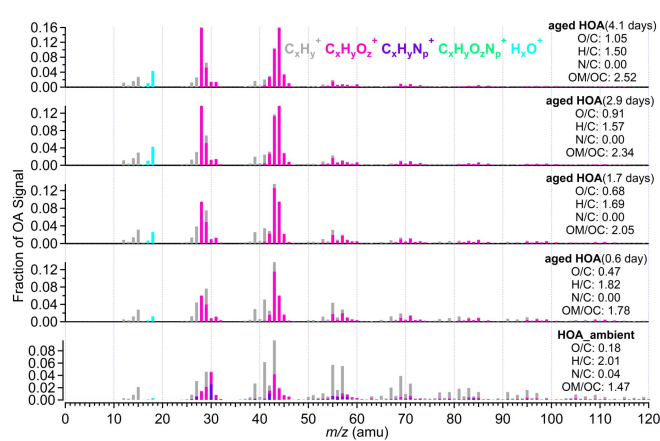
EPA1.1 days $\theta$ angles	deep-frying chicken	stir-frying cabbage	shallow-frying tofu	Kung Pao chicken
deep-frying chicken	<b>0</b>	<b>20</b>	<b>17</b>	<b>15</b>
stir-frying cabbage		<b>0</b>	<b>10</b>	<b>14</b>
shallow-frying tofu			<b>0</b>	<b>16</b>
Kung Pao chicken				<b>0</b>

EPA2.1 days $\theta$ angles	deep-frying chicken	stir-frying cabbage	shallow-frying tofu	Kung Pao chicken
deep-frying chicken	<b>0</b>	<b>22</b>	<b>18</b>	<b>17</b>
stir-frying cabbage		<b>0</b>	<b>10</b>	<b>13</b>
shallow-frying tofu			<b>0</b>	<b>12</b>
Kung Pao chicken				<b>0</b>

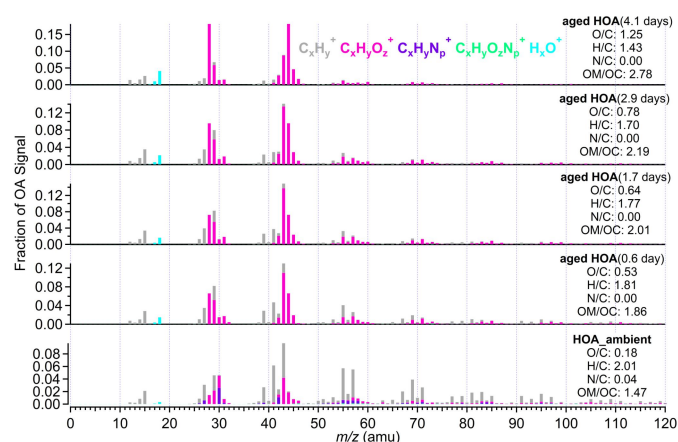




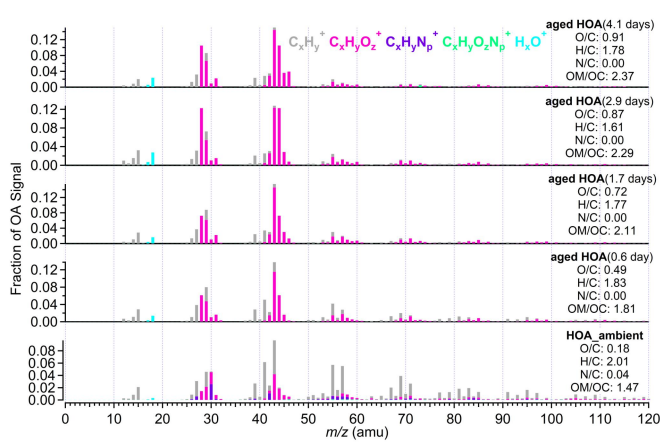
(a) 1500rpm\_16Nm



(b) 1750rpm\_16Nm



(c) 2000rpm\_32Nm



(d) 2000rpm\_40Nm

Fig.S4. The changes in mass spectra of aged HOA emissions from different conditions.

Table S7. The  $\theta$  angles among the mass spectra under different EPA at one vehicle condition (1500rpm\_16Nm, 1750rpm\_16Nm, 2000rpm\_16Nm, 2000rpm\_32Nm, and 2000rpm\_40Nm, respectively).

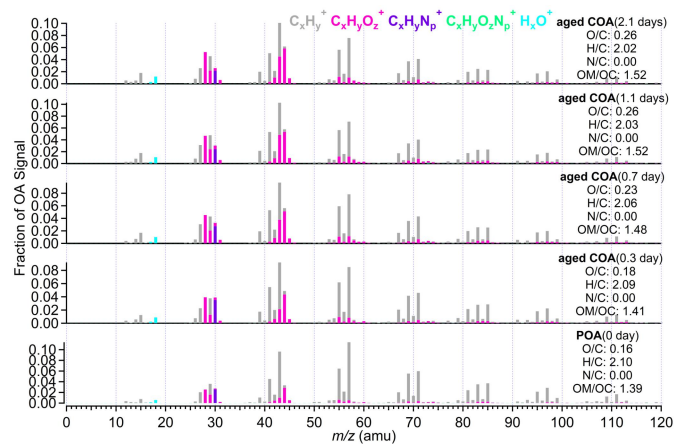
1500rpm_16Nm $\theta$ angles	HOA_ambient	0.6 day	1.7 days	2.9 days	4.1 days
HOA_ambient	0	27	45	63	63
0.6 day		0	24	46	46
1.7 days			0	22	22
2.9 days				0	1
4.1 days					0

1750rpm_16Nm $\theta$ angles	HOA_ambient	0.6 day	1.7 days	2.9 days	4.1 days
HOA_ambient	0	29	40	51	57
0.6 day		0	14	29	35
1.7 days			0	15	21
2.9 days				0	7
4.1 days					0

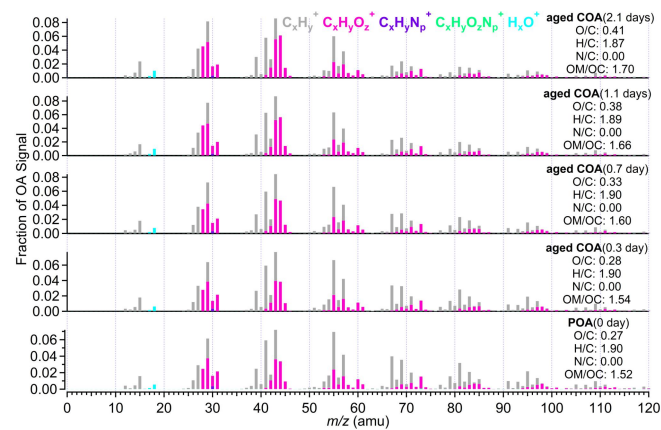
2000rpm_16Nm $\theta$ angles	HOA_ambient	0.6 day	1.7 days	2.9 days	4.1 days
HOA_ambient	0	29	40	51	57
0.6 day		0	15	29	36
1.7 days			0	15	22
2.9 days				0	7
4.1 days					0

2000rpm_32Nm $\theta$ angles	HOA_ambient	0.6 day	1.7 days	2.9 days	4.1 days
HOA_ambient	0	30	35	41	62
0.6 day		0	7	13	38
1.7 days			0	10	37
2.9 days				0	28
4.1 days					0

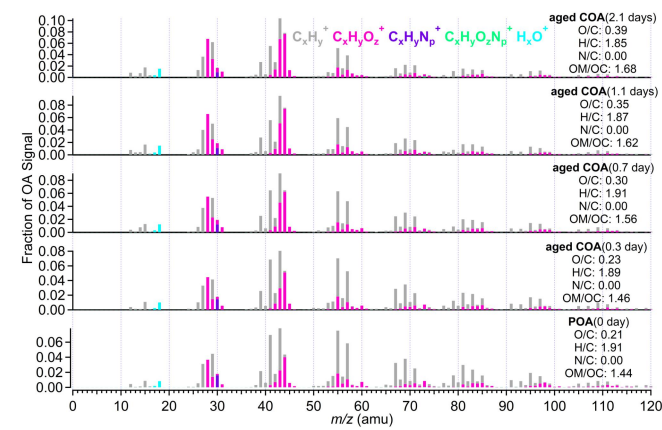
2000rpm_40Nm $\theta$ angles	HOA_ambient	0.6 day	1.7 days	2.9 days	4.1 days
HOA_ambient	0	29	36	48	46
0.6 day		0	10	24	21
1.7 days			0	19	13
2.9 days				0	12
4.1 days					0



(a) Deep-frying chicken



(b) Stir-frying cabbage



(c) Kung Pao chicken

Fig.S5. The mass spectra of aged COA oxidation under different OH exposure for different Chinese dishes.

Table S8. The  $\theta$  angles among the mass spectra under different EPA for different Chinese dishes.

<b>Deep-frying chicken</b>	POA	0.3 day	0.7 day	1.1 days	2.1 days
POA	0	12	17	19	19
0.3 day		0	6	9	9
0.7 day			0	4	5
1.1 days				0	4
2.1 days					0

<b>Stir-frying cabbage</b>	POA	0.3 day	0.7 day	1.1 days	2.1 days
POA	0	5	10	15	18
0.3 day		0	6	10	14
0.7 day			0	6	9
1.1 days				0	5
2.1 days					0

<b>Shallow frying tofu</b>	POA	0.3 day	0.7 day	1.1 days	2.1 days
POA	0	7	12	15	21
0.3 day		0	6	9	14
0.7 day			0	3	9
1.1 days				0	6
2.1 days					0

<b>Kung Pao chicken</b>	POA	0.3 day	0.7 day	1.1 days	2.1 days
POA	0	7	13	19	23
0.3 day		0	8	13	17
0.7 day			0	7	10
1.1 days				0	7
2.1 days					0

146  
147

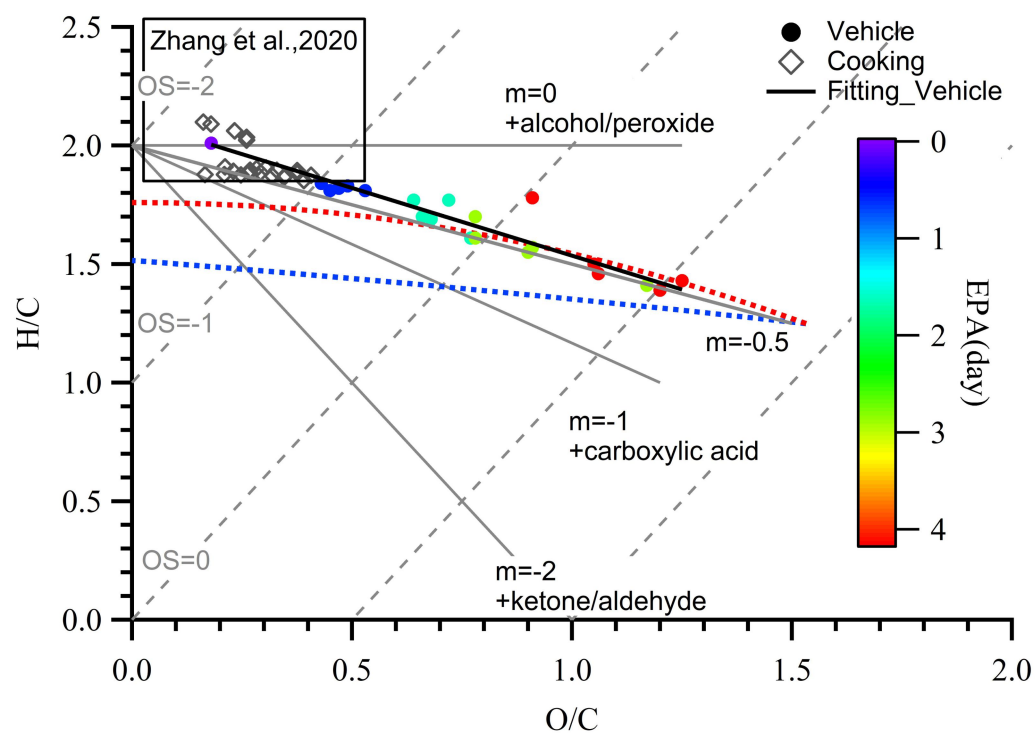


Fig.S6. Van Krevelen diagram of POA, aged COA and aged HOA from vehicle and cooking.

148  
149  
150

151  
152

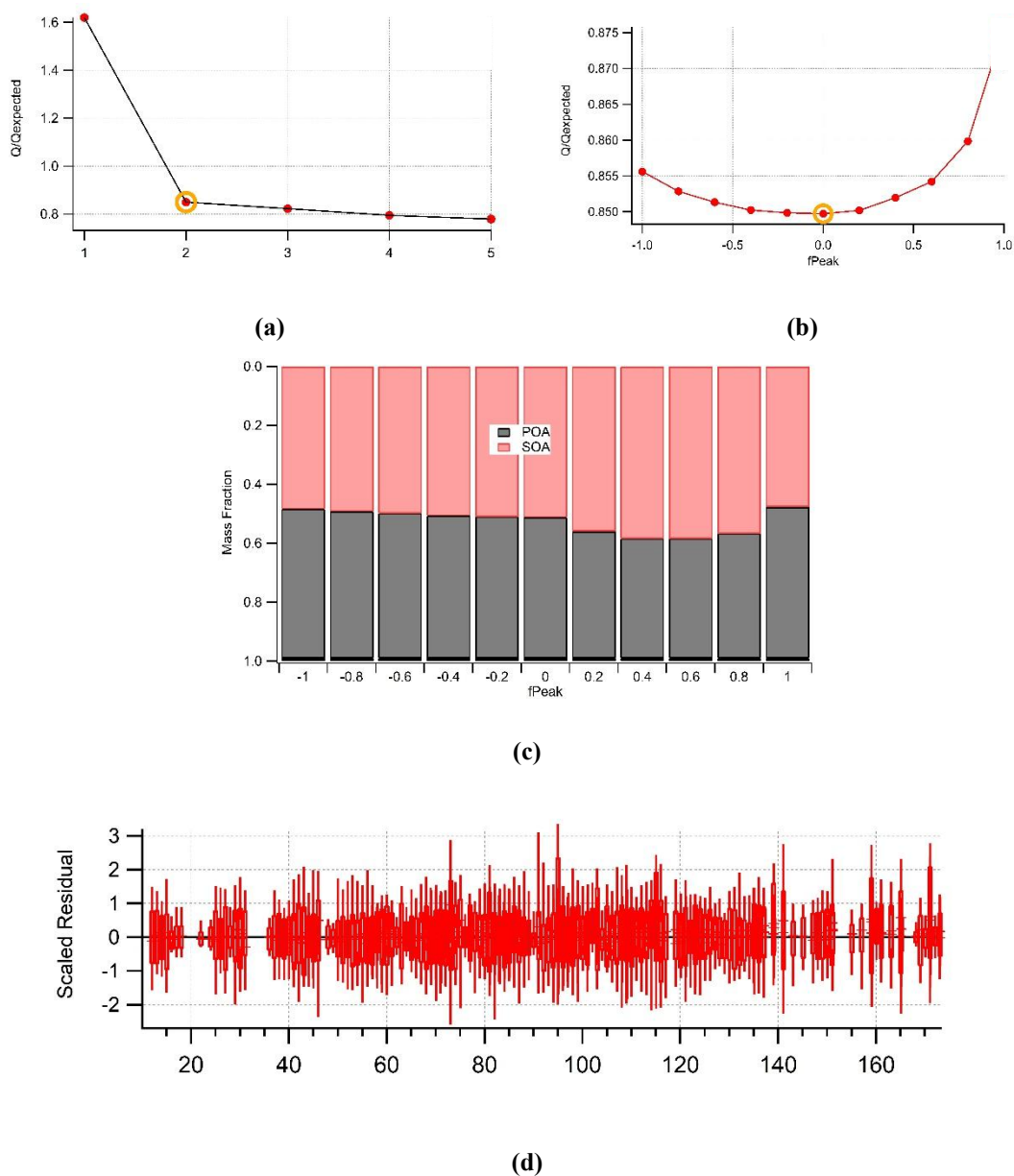


Fig.S7. Diagnostic plots of the PMF analysis on OA mass spectral matrix for stir-frying cabbage. (a)  $Q/Q_{exp}$  as a function of number of factors ( $P$ ) selected for PMF modeling. For the four-factor solution (i.e., the best  $P$ ), (b)  $Q/Q_{exp}$  as a function of  $f_{Peak}$ , (c) The fractions of OA factors vs.  $f_{Peak}$ , (d) The  $Q/Q_{exp}$  values for each  $m/z$

154  
155

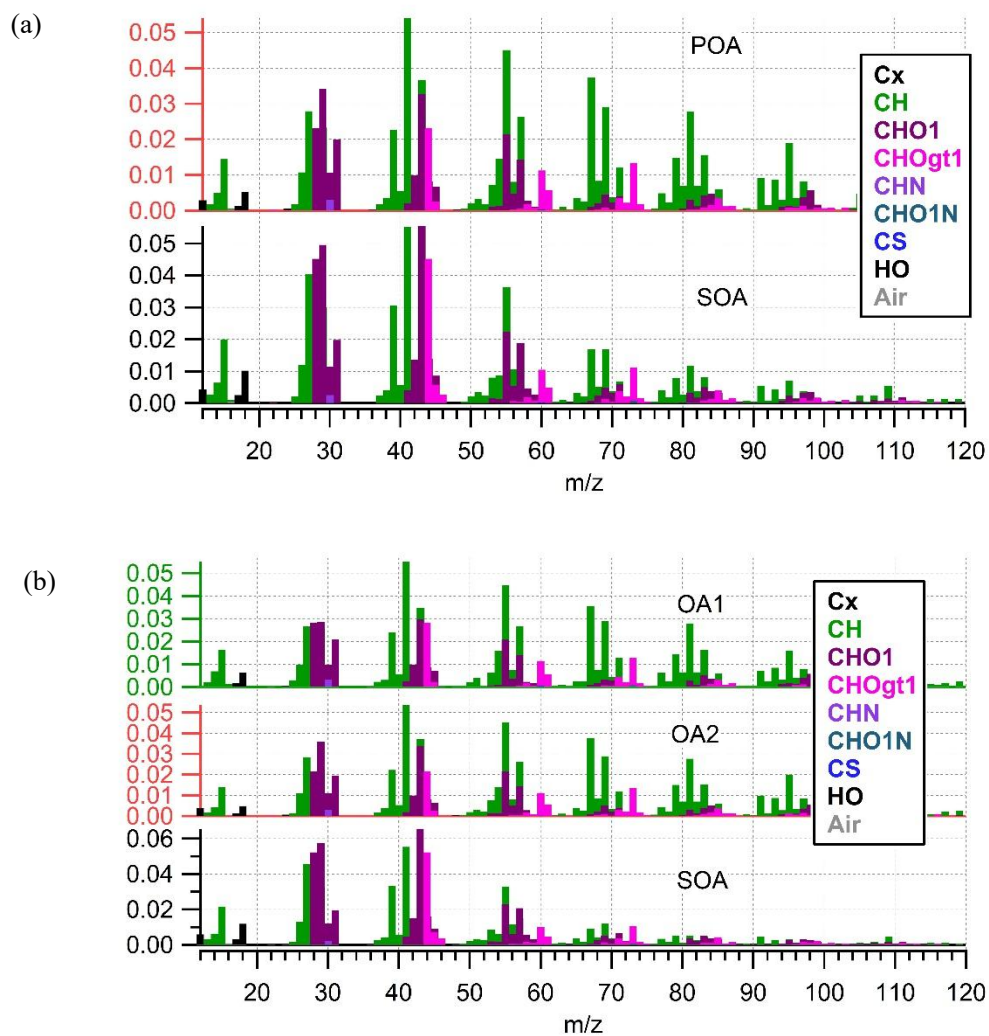


Fig.S8. Mass spectra of the (a) 2-factor, and (b) 3-factor solution using PMF method in stir-frying cabbage OA analysis.

157  
158  
  
  
159  
160  
161

Table S9. The optimum choices for PMF factors in stir-frying cabbage OA analysis.

Factor number	Fpeak	Seed	Q/Q <sub>exp</sub>	Solution Description
1	0	0	1.62	Too few factors, large residuals at time series and key m/z
2	0	0	0.85	<b>Optimum choices for PMF factors (POA and SOA). Time series, mass spectra and diurnal variations of PMF factors are reasonable.</b>
3-5	0	0	0.77-0.82	Factor split. Take 3 factor number solution as an example, POA was split into two factors with similar spectra.



162  
163

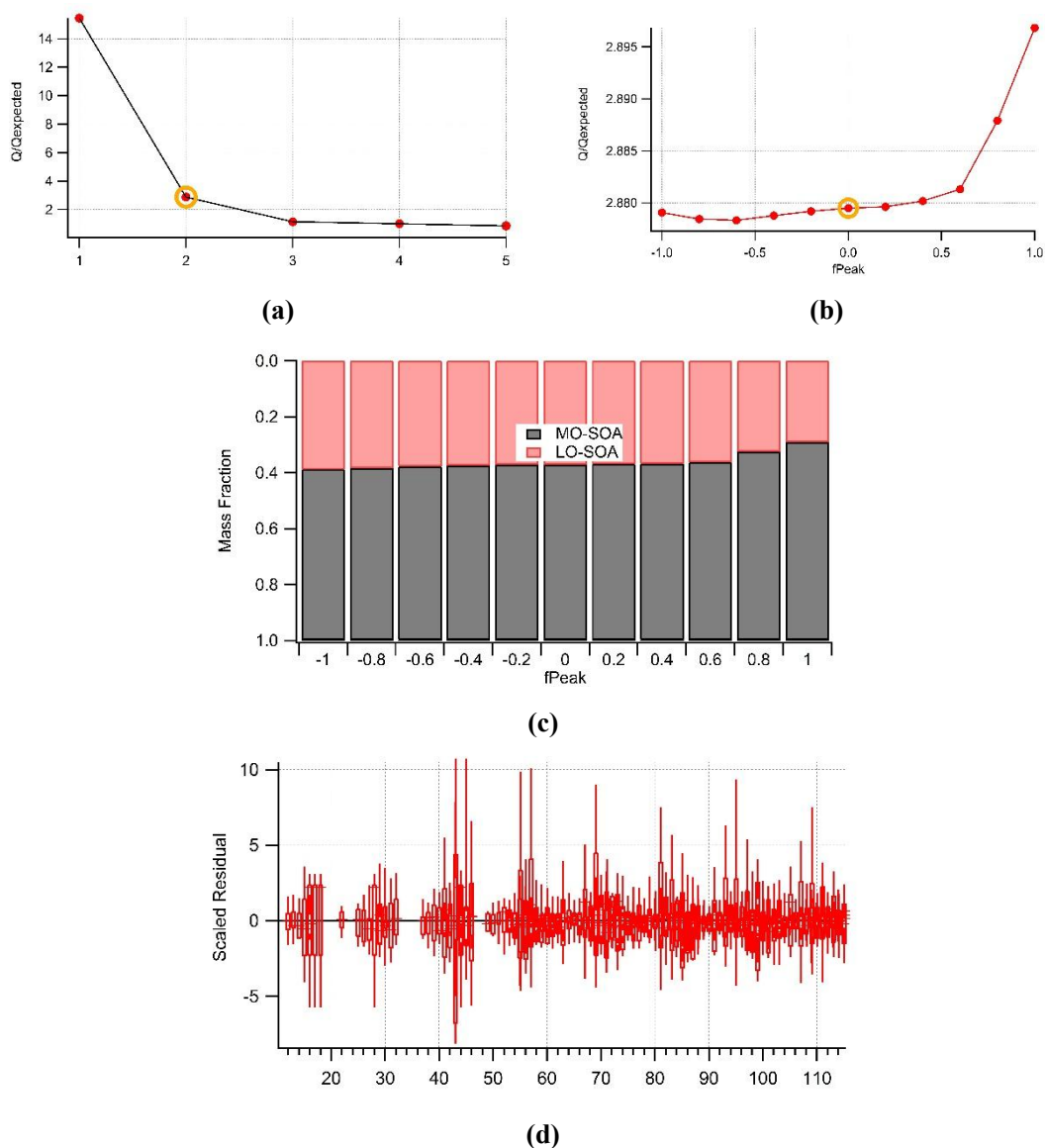


Fig.S9. Diagnostic plots of the PMF analysis on aged HOA mass spectral matrix for 2000rpm\_32Nm. (a)  $Q/Q_{exp}$  as a function of number of factors (P) selected for PMF modeling. For the four-factor solution (i.e., the best P), (b)  $Q/Q_{exp}$  as a function of  $f_{Peak}$ , (c) The fractions of OA factors vs.  $f_{Peak}$ , (d) The  $Q/Q_{exp}$  values for each  $m/z$

164  
165

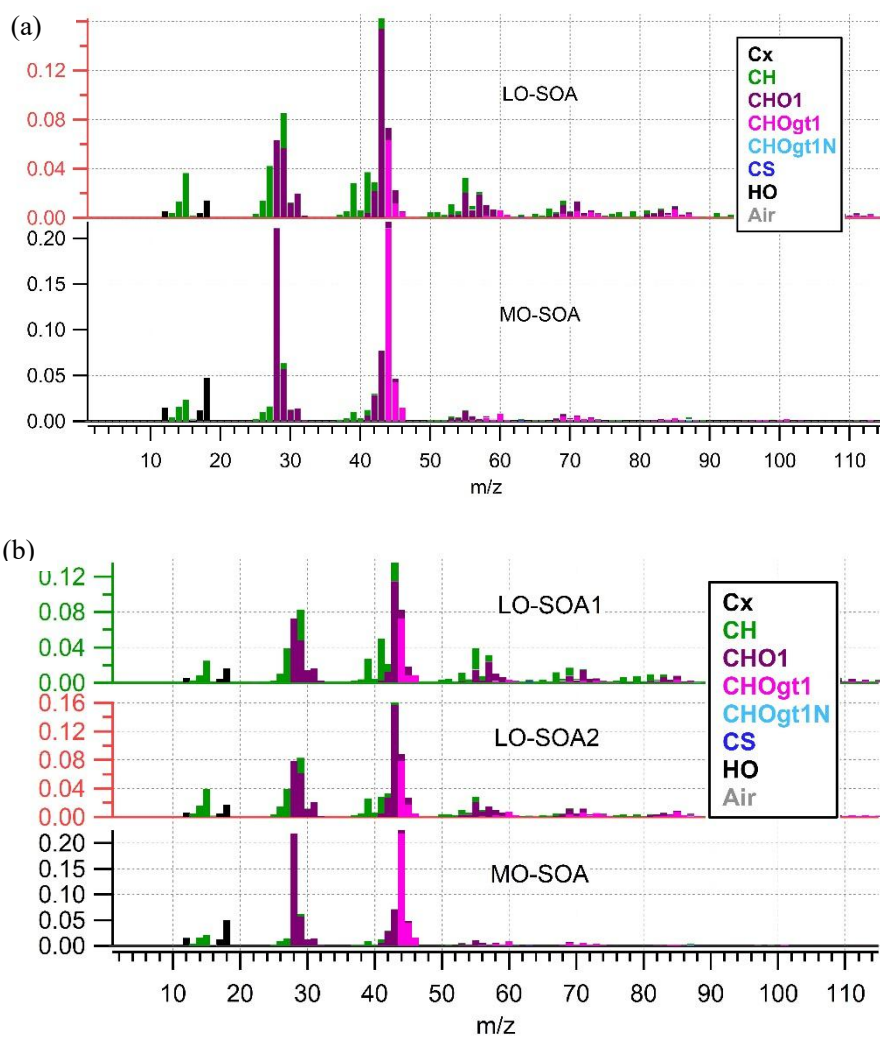


Fig.S10. Mass spectra of the (a) 2-factor, and (b) 3-factor solution using PMF method in 2000rpm\_32Nm aged HOA analysis.

Table S10. The optimum choices for PMF factors in 2000rpm\_32Nm aged HOA analysis.

Factor number	F <sub>peak</sub>	Seed	Q/Q <sub>exp</sub>	Solution Description
1	0	0	15.44	Too few factors, large residuals at time series and key m/z
2	0	0	2.87	<b>Optimum choices for PMF factors (LO-SOA and MO-SOA). Time series, mass spectra and diurnal variations of PMF factors are reasonable.</b>
3-5	0	0	0.85-1.14	Factor split. Take 3 factor number solution as an example, LO-SOA was split into two factors with similar spectra.

177

178 Table S11. A summary of dominant peaks among cooking PMF POA.

	Deep-frying chicken	Stir-frying cabbage	Shallow frying tofu	Kung Pao chicken
$f_{41}$	0.0508	0.0560	0.0682	0.0685
$f_{43}$	0.0802	0.0365	0.0489	0.0597
$f_{55}$	0.0641	0.0664	0.0842	0.0757
$f_{57}$	0.0966	0.0411	0.0473	0.0612
$f_{67}$	0.0211	0.0382	0.0404	0.0333
$f_{69}$	0.0486	0.0343	0.0383	0.0376

179

180 Table S12. A summary of dominant peaks among cooking PMF SOA.

	Deep-frying chicken	Stir-frying cabbage	Shallow frying tofu	Kung Pao chicken
$f_{28}$	0.0504	0.0451	0.0463	0.0682
$f_{29}$	0.0481	0.0796	0.0675	0.0644
$f_{41}$	0.0501	0.0590	0.0679	0.0547
$f_{43}$	0.1032	0.0865	0.0944	0.1023
$f_{44}$	0.0609	0.0596	0.0584	0.0800
$f_{55}$	0.0534	0.0586	0.0636	0.0495
$f_{57}$	0.0665	0.0376	0.0421	0.0364

181

182 Table S13. A summary of dominant peaks among vehicle PMF LO-SOA.

	1500rpm_16Nm	1750rpm_16Nm	2000rpm_16Nm	2000rpm_32Nm	2000rpm_40Nm
$f_{28}$	0.0579	0.0551	0.0527	0.0493	0.0081
$f_{41}$	0.0417	0.0493	0.0443	0.0386	0.0574
$f_{43}$	0.1571	0.1495	0.1523	0.1670	0.1632
$f_{44}$	0.0663	0.0653	0.0623	0.0597	0.0183
$f_{55}$	0.0384	0.0393	0.0386	0.0339	0.0447
$f_{57}$	0.0246	0.0270	0.0253	0.0226	0.0329

183

184 Table S14. A summary of dominant peaks among vehicle PMF MO-SOA.

	1500rpm_16Nm	1750rpm_16Nm	2000rpm_16Nm	2000rpm_32Nm	2000rpm_40Nm
$f_{28}$	0.2077	0.1590	0.2141	0.2049	0.1099
$f_{41}$	0.0139	0.0186	0.0124	0.0124	0.0242
$f_{43}$	0.0722	0.1063	0.0777	0.0771	0.1431
$f_{44}$	0.2190	0.1688	0.2239	0.2126	0.1208
$f_{55}$	0.0127	0.0181	0.0120	0.0120	0.0238
$f_{57}$	0.0042	0.0076	0.0026	0.0032	0.0127

185

186

187

188

189 Table S15. The  $\theta$  angles among the mass spectra of cooking PMF SOA for different dishes.

cooking SOA $\theta$ angles	deep-frying chicken	stir-frying cabbage	shallow-frying tofu	Kung Pao chicken
deep-frying chicken	<b>0</b>	<b>21</b>	<b>18</b>	<b>19</b>
stir-frying cabbage		<b>0</b>	<b>8</b>	<b>13</b>
shallow-frying tofu			<b>0</b>	<b>13</b>
Kung Pao chicken				<b>0</b>

190

191 Table S16. The  $\theta$  angles among the mass spectra of cooking PMF POA for different dishes.

cooking POA $\theta$ angles	deep-frying chicken	stir-frying cabbage	shallow-frying tofu	Kung Pao chicken
deep-frying chicken	<b>0</b>	<b>31</b>	<b>28</b>	<b>20</b>
stir-frying cabbage		<b>0</b>	<b>13</b>	<b>17</b>
shallow-frying tofu			<b>0</b>	<b>10</b>
Kung Pao chicken				<b>0</b>

192

193 Table S17. The  $\theta$  angles among the mass spectra of vehicle PMF LO-SOA at different conditions.

Vehicle LO-SOA $\theta$ angles	1500rpm_16Nm	1750rpm_16Nm	2000rpm_16Nm	2000rpm_32Nm	2000rpm_40Nm
1500rpm_16Nm	<b>0</b>	<b>3</b>	<b>3</b>	<b>6</b>	<b>19</b>
1750rpm_16Nm		<b>0</b>	<b>3</b>	<b>7</b>	<b>3</b>
2000rpm_16Nm			<b>0</b>	<b>6</b>	<b>3</b>
2000rpm_32Nm				<b>0</b>	<b>6</b>
2000rpm_40Nm					<b>0</b>

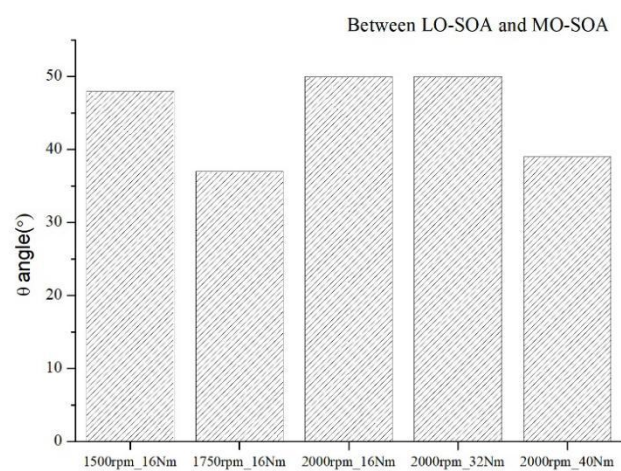
194

195 Table S18. The  $\theta$  angles among the mass spectra of vehicle PMF MO-SOA at different conditions.

Vehicle MO-SOA $\theta$ angles	1500rpm_16Nm	1750rpm_16Nm	2000rpm_16Nm	2000rpm_32Nm	2000rpm_40Nm
1500rpm_16Nm	<b>0</b>	<b>12</b>	<b>2</b>	<b>2</b>	<b>29</b>
1750rpm_16Nm		<b>0</b>	<b>12</b>	<b>11</b>	<b>17</b>
2000rpm_16Nm			<b>0</b>	<b>3</b>	<b>28</b>
2000rpm_32Nm				<b>0</b>	<b>27</b>
2000rpm_40Nm					<b>0</b>

196

197



198

199 Fig.S11. The  $\theta$  angles between vehicle PMF LO-SOA and PMF MO-SOA under five running conditions.

200

201

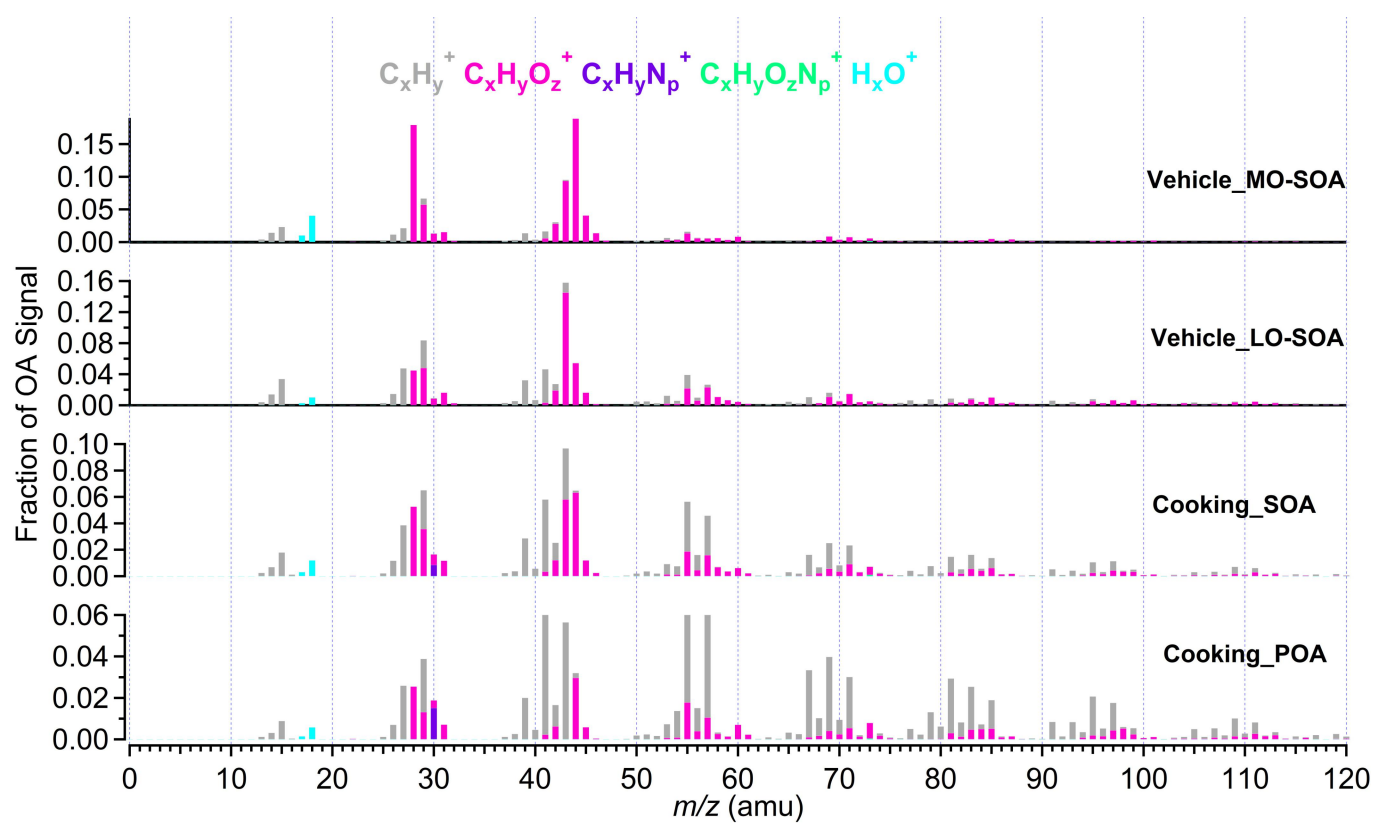


Fig.S12. Mass spectral profiles of cooking POA, cooking SOA, vehicle LO-SOA, and vehicle MO-SOA as the primary and secondary spectrum constraints in ME-2 model.

207

208

Table S19. The  $\theta$  angles between ambient COA, HOA, LO-OOA and MO-OOA factors and the cooking PMF POA, SOA, and the vehicle PMF LO-SOA, MO-SOA.

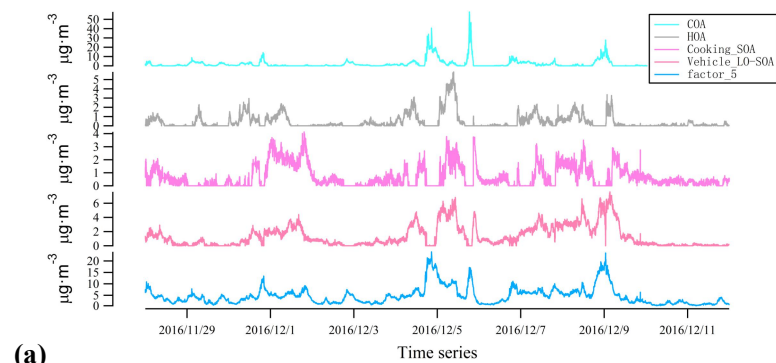
<b><math>\theta</math> angles</b>	HOA_ambient	COA_ambient	LO-OOA_ambient	MO-OOA_ambient	Cooking_POA	Cooking_SOA	Vehicle_LO-SOA	Vehicle_MO-SOA
HOA_ambient	<b>0</b>	21	36	56	21	27	30	61
COA_ambient	21	<b>0</b>	31	49	18	22	34	55
LO-OOA_ambient	36	31	<b>0</b>	37	18	28	32	52
MO-OOA_ambient	56	49	37	<b>0</b>	18	28	33	18
Cooking_POA	21	18	18	18	<b>0</b>	31	39	64
Cooking_SOA	27	22	28	28	31	<b>0</b>	19	46
Vehicle_LO-SOA	30	34	32	33	39	19	<b>0</b>	46
Vehicle_MO-SOA	61	55	52	18	64	46	46	<b>0</b>

209

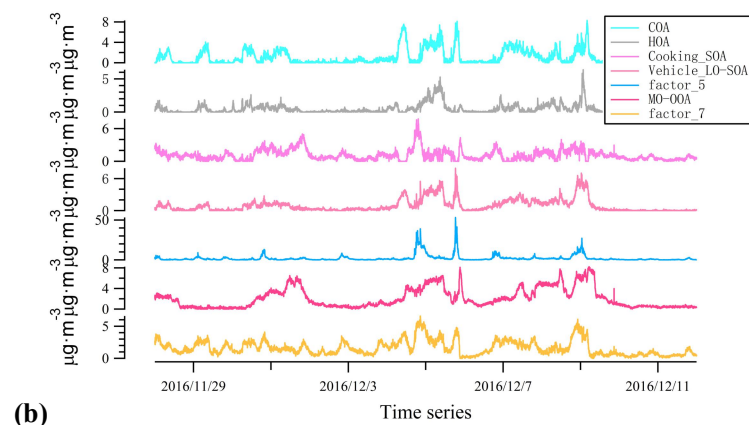
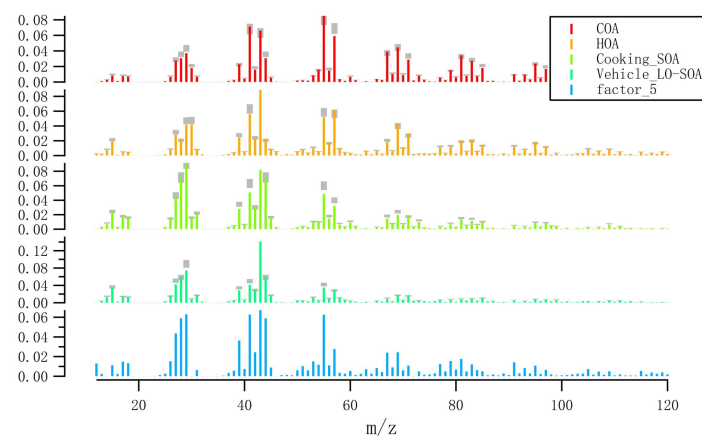
210

211





(a)



(b)

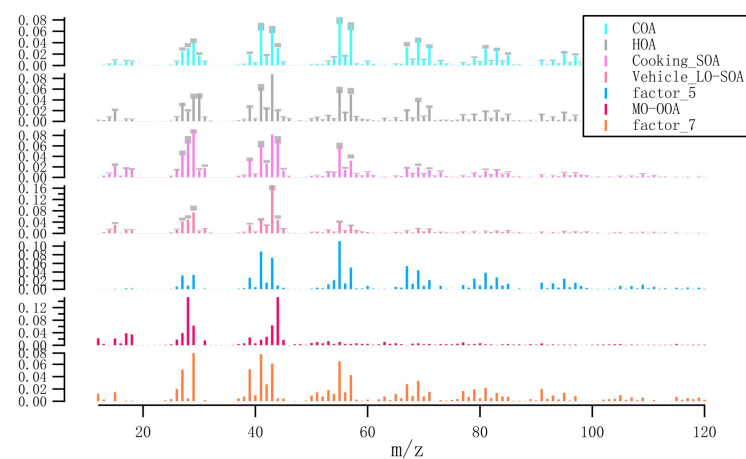
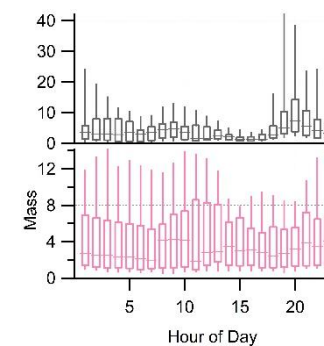
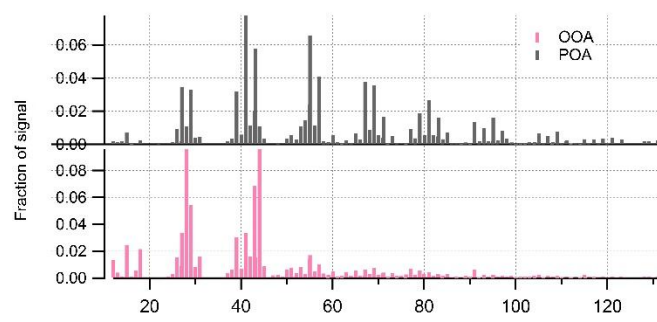
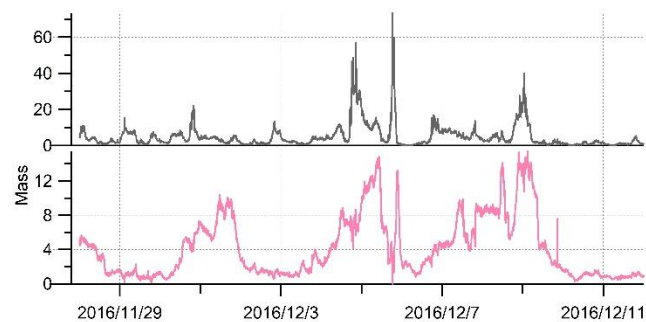
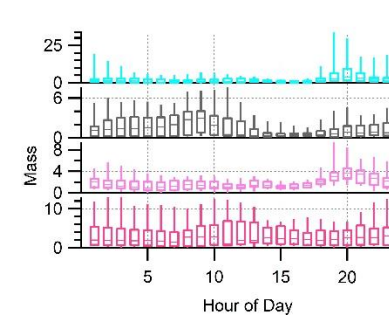
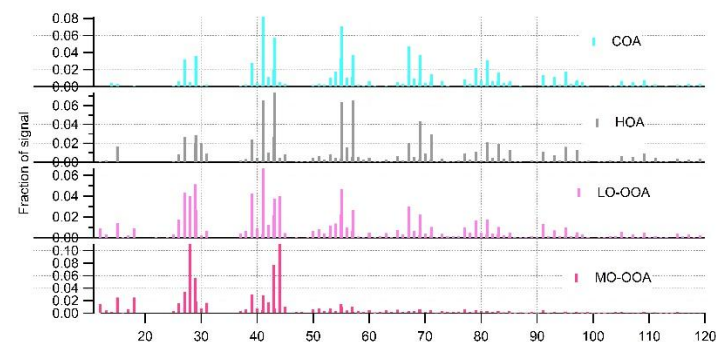
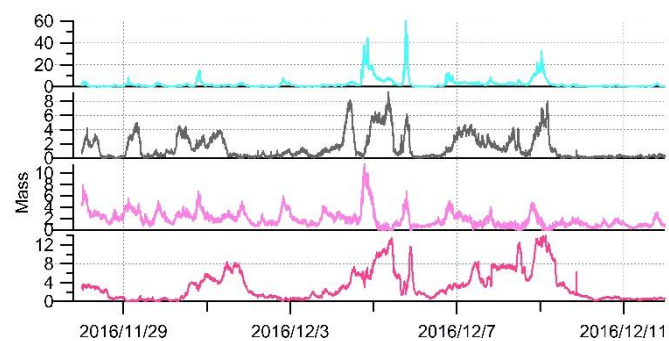


Fig.S13. (a) 5-factor solution performed by ME-2 on organic mass spectra; (b) 7-factor solution performed by ME-2 on organic mass spectra during the wintertime in Shanghai.



(a)



(b)

Fig.S14. (a) 2-factor solution performed by PMF on organic mass spectra during the wintertime in Shanghai; (b) 4-factor solution performed by PMF on organic mass spectra during the wintertime in Shanghai.

217  
218  
219  
220  
221  
222  
223  
224

Table S20. Pearson r between the factors identified by using PMF model (4-factor solution), and the external tracers during the wintertime observations in Shanghai.

Pearson r	Sulfate	CO <sub>2</sub> <sup>+</sup>	C <sub>2</sub> H <sub>4</sub> O <sub>2</sub> <sup>+</sup>	C <sub>10</sub> H <sub>8</sub> <sup>+</sup>
MO-OOA_PMF	0.89	0.96	0.67	0.61

Pearson r	Nitrate	C <sub>2</sub> H <sub>3</sub> O <sup>+</sup>	C <sub>6</sub> H <sub>10</sub> O <sup>+</sup>	C <sub>2</sub> H <sub>4</sub> O <sub>2</sub> <sup>+</sup>	C <sub>10</sub> H <sub>8</sub> <sup>+</sup>
LO-OOA_PMF	0.04	0.31	0.44	0.51	0.59

Pearson r	COA_PMF
C <sub>6</sub> H <sub>10</sub> O <sup>+</sup>	0.81

Pearson r	HOA_PMF
NO <sub>x</sub>	0.73

225

226

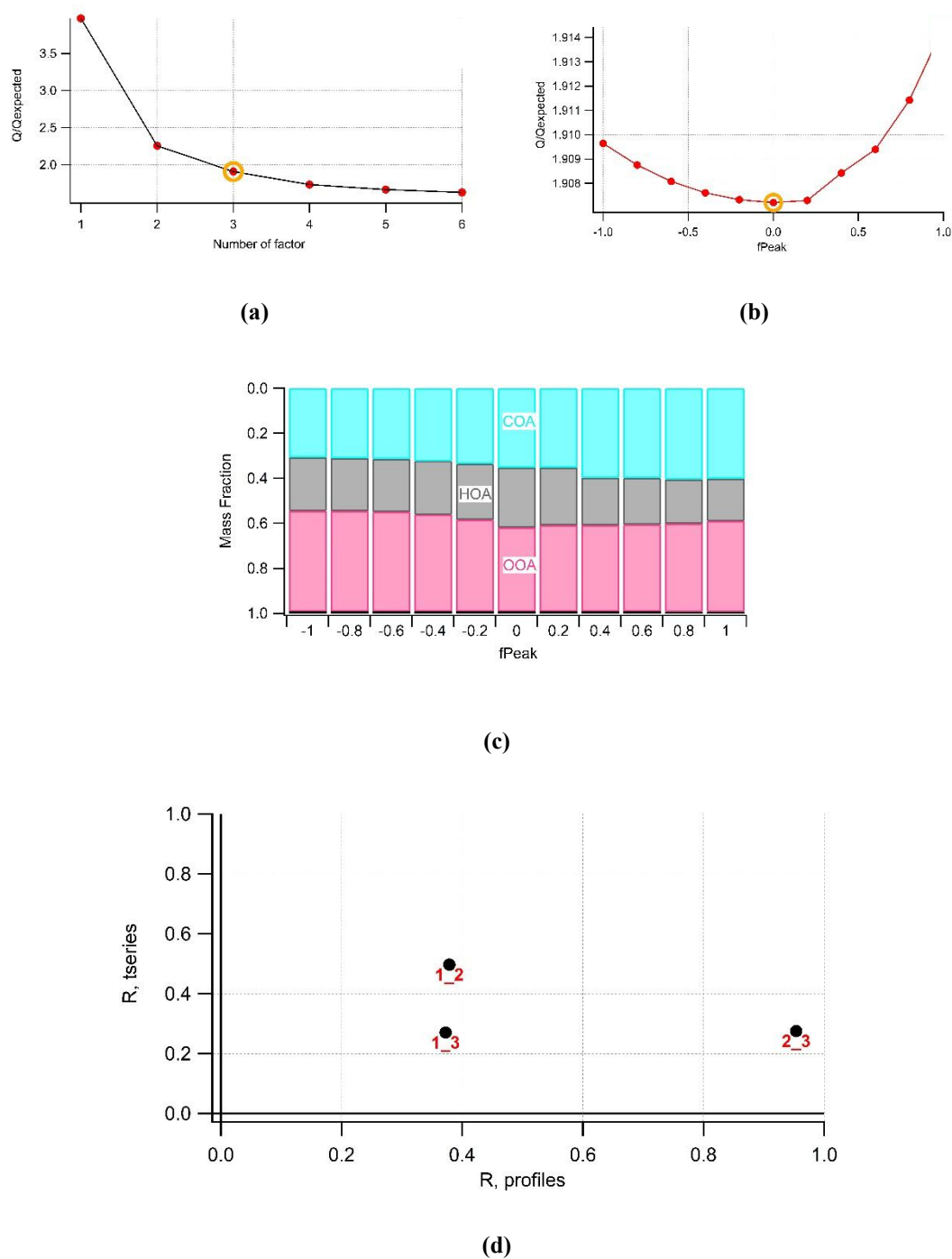


Fig.S15. Diagnostic plots of the PMF analysis on OA mass spectral matrix for the winter observation. (a)  $Q/Q_{exp}$  as a function of number of factors (P) selected for PMF modeling. For the four-factor solution (i.e., the best P), (b)  $Q/Q_{exp}$  as a function of  $f_{Peak}$ , (c) The fractions of OA factors vs.  $f_{Peak}$ , (d) The correlations among PMF factors.

227

228

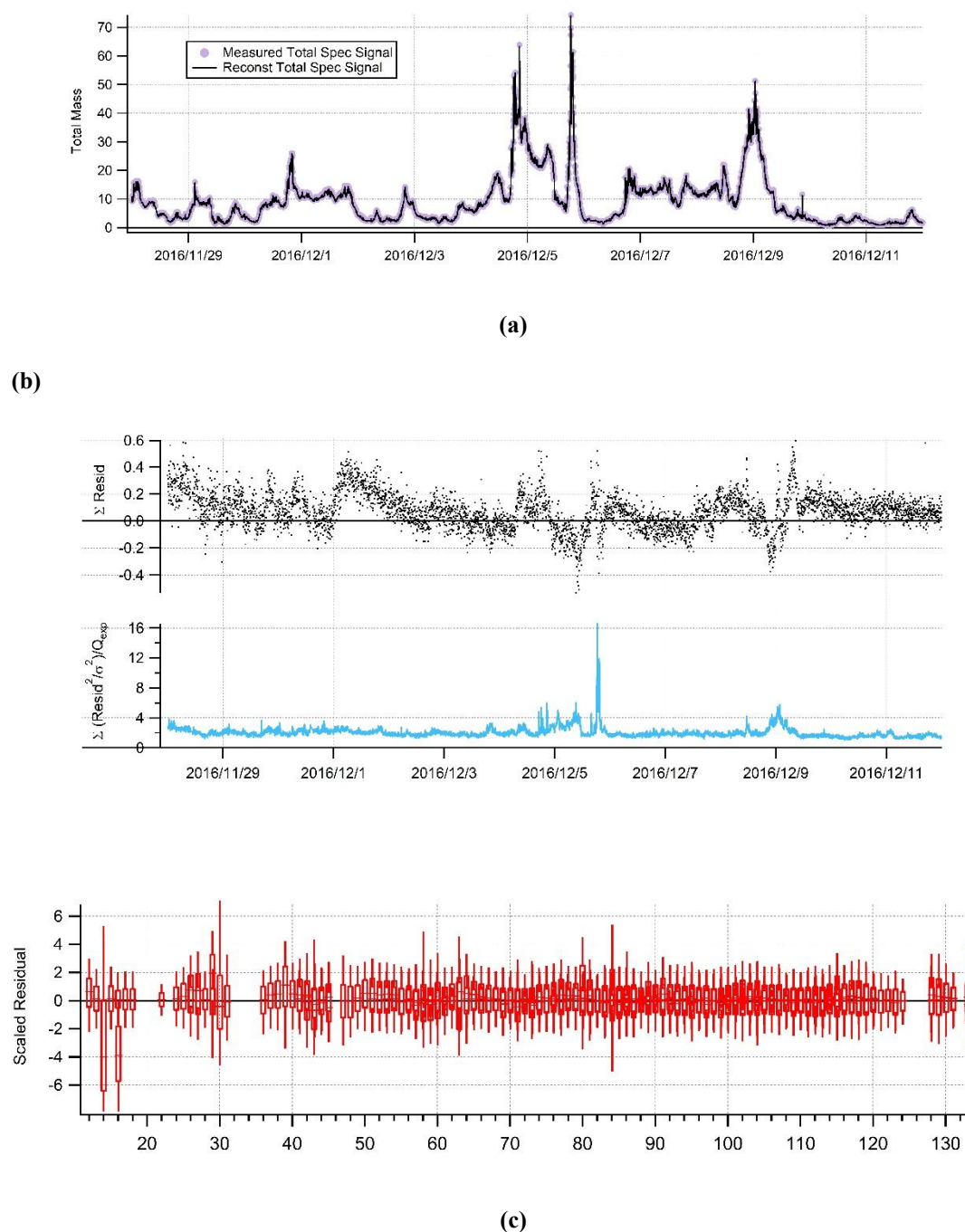


Fig.S16. Diagnostic plots of the PMF analysis on OA mass spectral matrix for the winter observation. (a) Time series of the measured organic mass and the reconstructed organic mass, (b) Variations of the residual (= measured – reconstructed) of the fit, and the  $Q/Q_{\text{exp}}$  for each point in time, and (c) The  $Q/Q_{\text{exp}}$  values for each  $m/z$

232  
233  
  
  
234  
235  
236  
237  
238  
239

Table S21. Descriptions of PMF solutions for organic aerosol in the winter study of Shanghai

Factor number	F <sub>peak</sub>	Seed	Q/Q <sub>exp</sub>	Solution Description
1	0	0	3.97	Too few factors, large residuals at time series and key m/z
2	0	0	2.26	Few factors (OOA- and HOA-like), large residuals at time series and key m/z. Factors are mixed to some extend based on the time series and spectra.
3	0	0	1.91	<b>Optimum choices for PMF factors (OOA, HOA and COA). Time series and diurnal variations of PMF factors are consistent with the external tracers. The spectra of four factors are consistent with the source spectra in AMS spectra database.</b>
4-6	0	0	1.63-1.73	Factor split. Take 4 factor number solution as an example, LO-OOA was split from other factors.

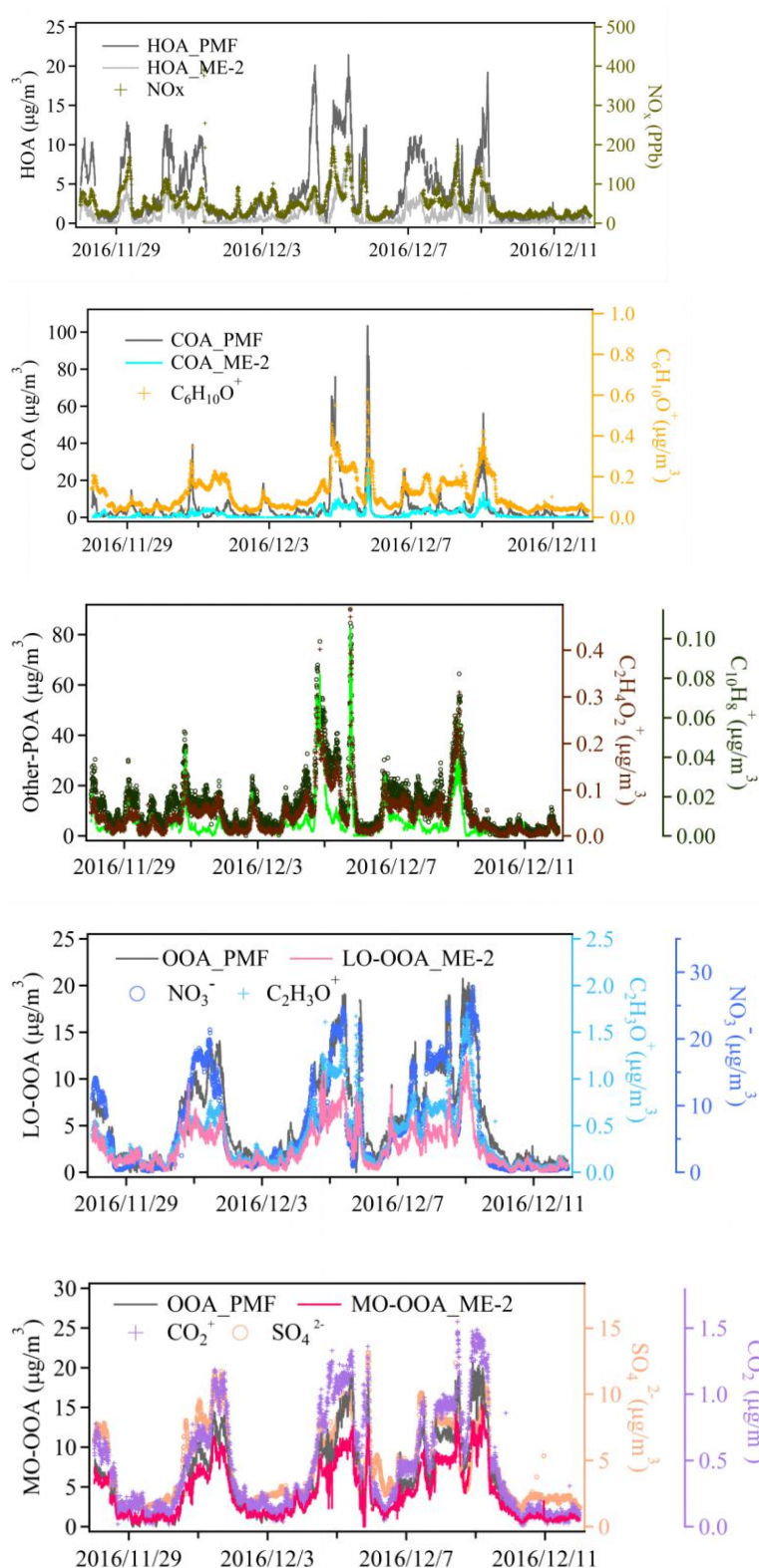


Fig.S17. The time-series correlations of all factors which resolved from PMF and ME-2 with external tracers during the wintertime observations in Shanghai.

241

242

243

244  
245  
246  
  
247  
  
248  
  
249  
  
250  
  
251  
252  
253

Table S22. Pearson r between the factors identified by using PMF and ME-2 model, and the external tracers during the wintertime observations in Shanghai.

Pearson r	Sulfate	CO <sub>2</sub> <sup>+</sup>	C <sub>2</sub> H <sub>4</sub> O <sub>2</sub> <sup>+</sup>	C <sub>10</sub> H <sub>8</sub> <sup>+</sup>
OOA_PMF	0.90	0.96	0.65	0.96
MO-OOA_ME-2	0.87	0.95	0.61	0.55

Pearson r	Nitrate	C <sub>2</sub> H <sub>3</sub> O <sup>+</sup>
OOA_PMF	0.94	0.90
LO-OOA_ME-2	0.84	0.95

Pearson r	COA_PMF	COA_ME-2
C <sub>6</sub> H <sub>10</sub> O <sup>+</sup>	0.74	0.85

Pearson r	HOA_PMF	HOA_ME-2
NO <sub>x</sub>	0.70	0.64

Pearson r	C <sub>2</sub> H <sub>4</sub> O <sub>2</sub> <sup>+</sup>	C <sub>10</sub> H <sub>8</sub> <sup>+</sup>
Other POA_ME-2	0.88	0.88



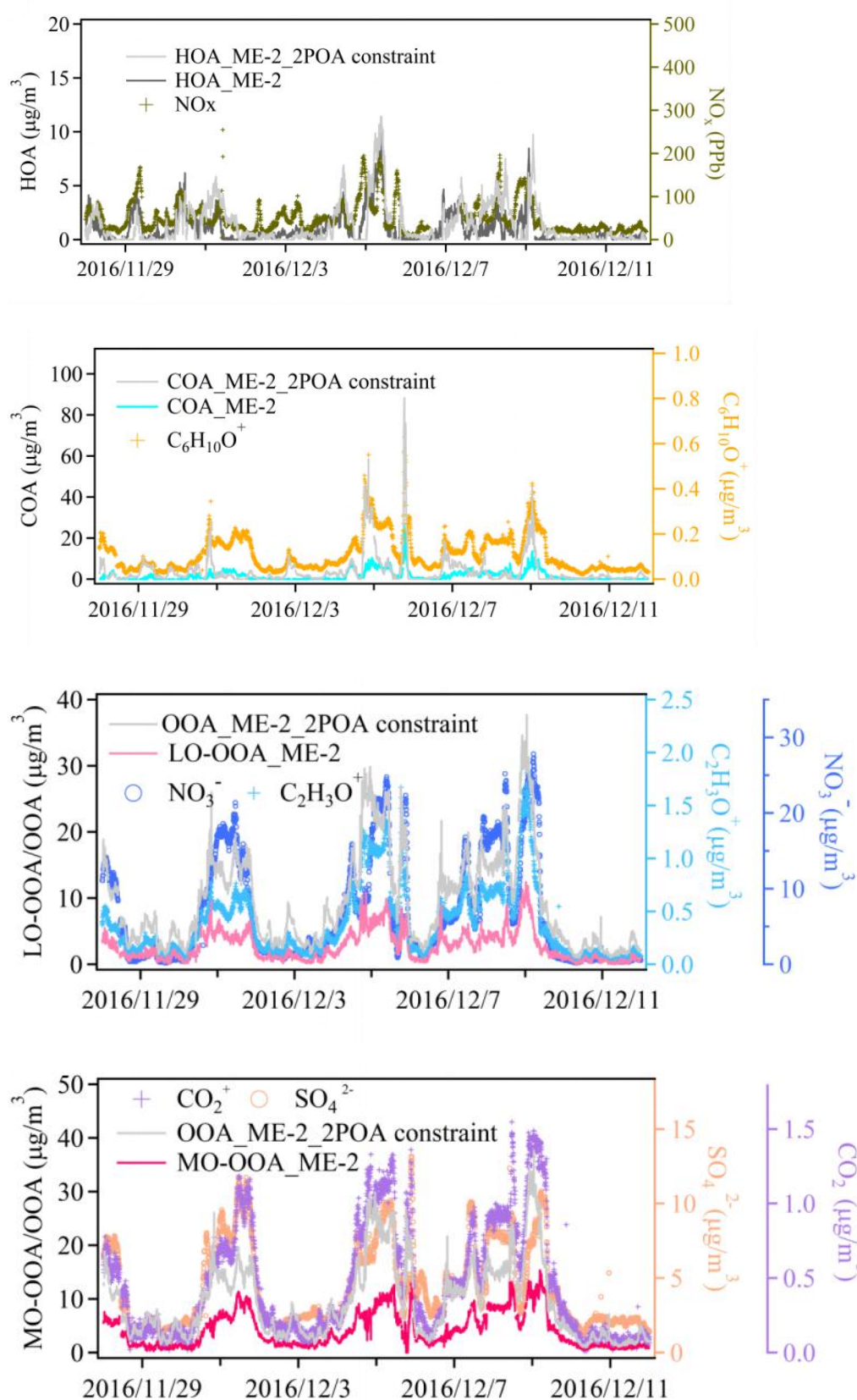


Fig. S18. The time-series correlations of all factors which resolved from ME-2 constraining two POA profiles and ME-2 constraining four factors spectral profiles with external tracers during the wintertime observations in Shanghai.

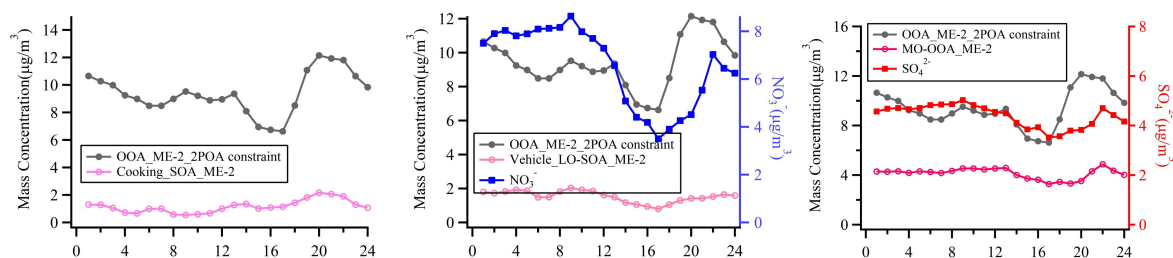
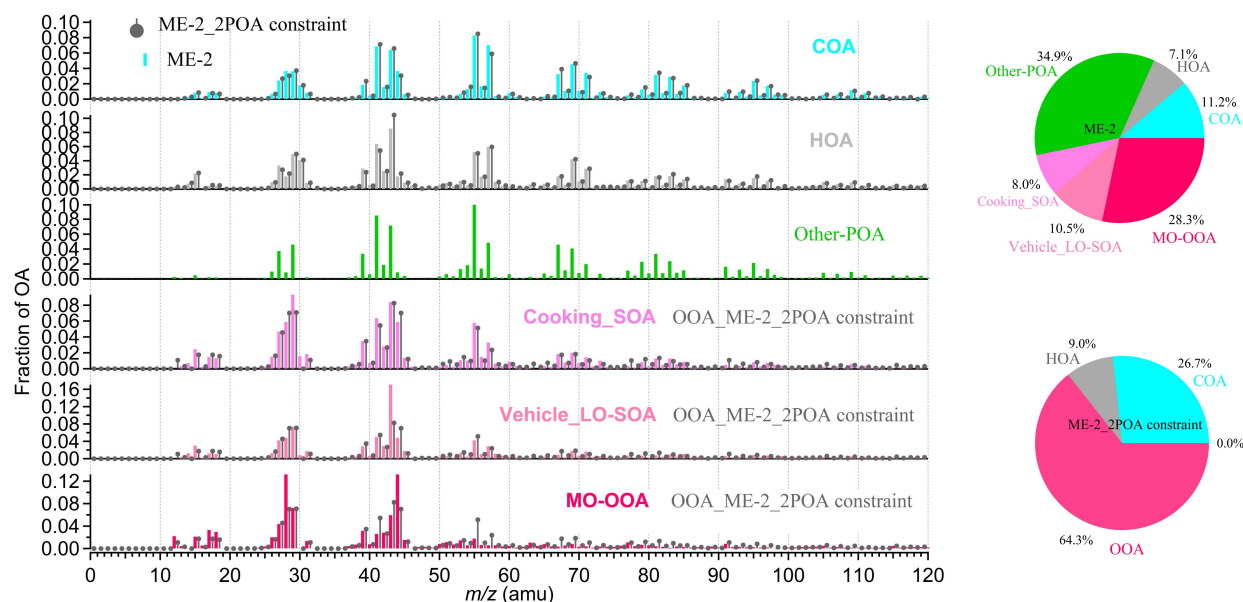
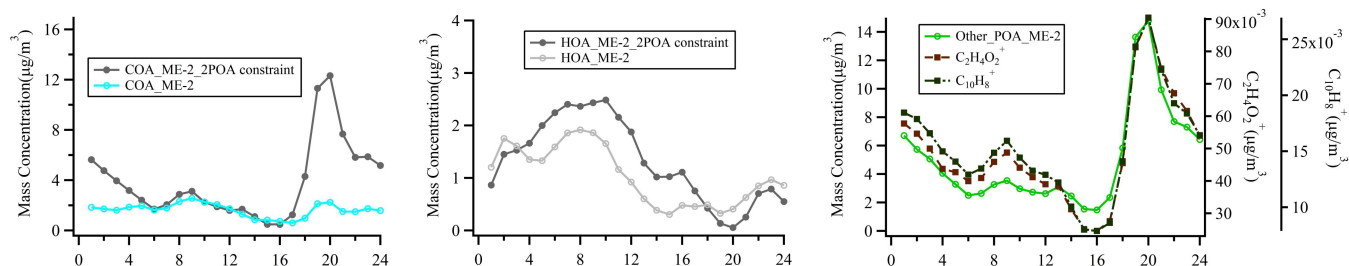


Fig.S19. The comparison of the mass spectra, the diurnal variation, and fraction between ME-2 constraining the spectral profiles of two primary factors (the cooking POA, ambient HOA) and ME-2 constraining four spectral profiles resolved factors during the wintertime in Shanghai. The black lines in the spectra and diurnal pattern are the result of ME-2 analysis by constraining two spectral profiles in the actual atmosphere in Shanghai winter. The four spectral profiles were two primary OA factors (the cooking POA, ambient HOA resolved in three cities) and two secondary OA factors (the cooking SOA, the vehicle LO-SOA).

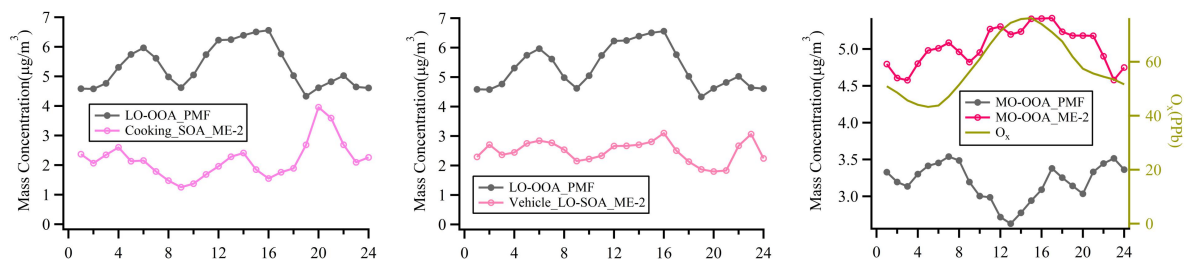
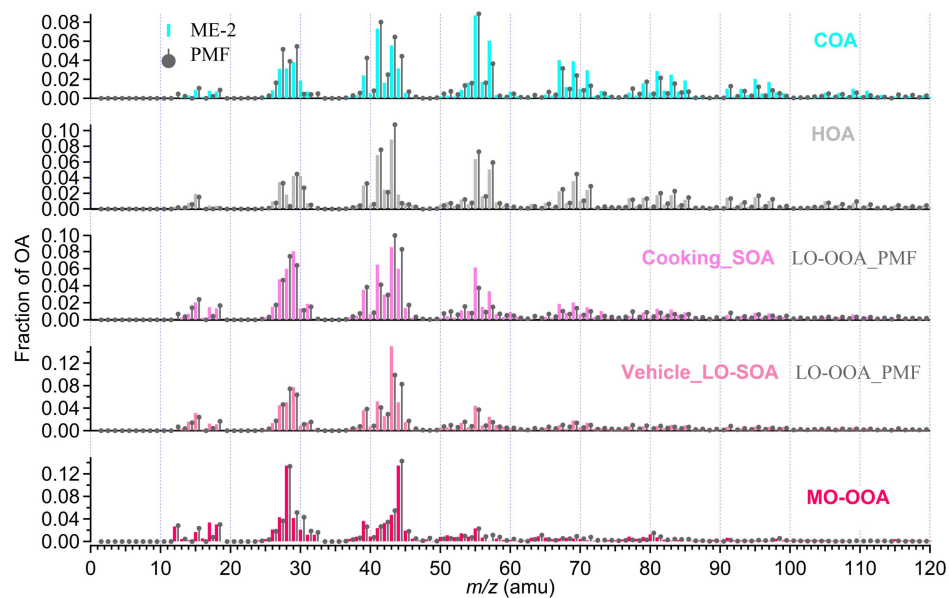
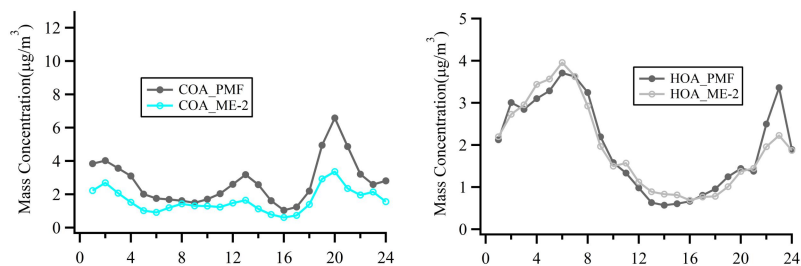


Fig.S20. The comparison of the mass spectra, the diurnal variation, and fraction between ME-2 and PMF resolved factors during the summertime in Shanghai.

279  
280

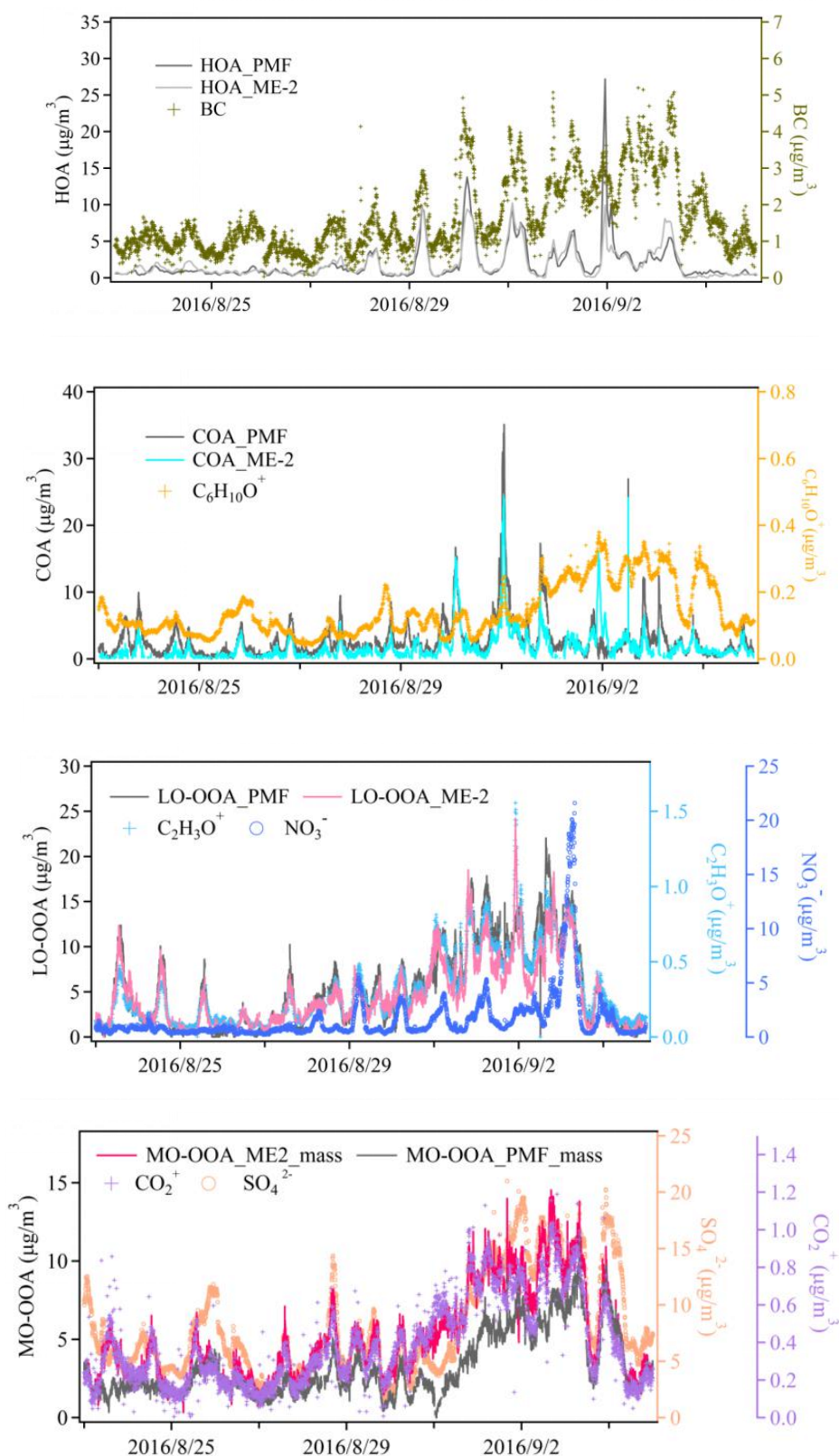


Fig. S21. The time-series correlations of all factors which resolved from PMF and ME-2 with external tracers during the summertime observations in Shanghai.

281  
282

Table S23. Pearson r between the factors identified by using PMF and ME-2 model, and the external tracers during the summertime observations in Shanghai.

Pearson r	Sulfate	CO <sub>2</sub> <sup>+</sup>
MO-OOA_PMF	0.94	0.79
MO-OOA_ME-2	0.87	0.95

Pearson r	Nitrate	C <sub>2</sub> H <sub>3</sub> O <sup>+</sup>
LO-OOA_PMF	0.53	0.94
LO-OOA_ME-2	0.60	0.96

Pearson r	COA_PMF	COA_ME-2
C <sub>6</sub> H <sub>10</sub> O <sup>+</sup>	0.23	0.36

Pearson r	HOA_PMF	HOA_ME-2
BC	0.52	0.55